

# Shapley Optical Survey II: The effect of environment on the colour-magnitude relation and galaxy colours<sup>\*</sup>

C. P. Haines,<sup>1\*\*</sup> P. Merluzzi,<sup>1</sup> A. Mercurio,<sup>1</sup> A. Gargiulo,<sup>1</sup> N. Krusanova,<sup>1</sup>  
G. Busarello,<sup>1</sup> F. La Barbera,<sup>1</sup> and M. Capaccioli<sup>1,2</sup>

<sup>1</sup>INAF - Osservatorio Astronomico di Capodimonte, via Moiariello 16, I-80131 Napoli, Italy

<sup>2</sup>Department of Physics, Università “Federico II”, Napoli, Italy

Accepted 1988 December 15. Received 1988 December 14; in original form 1988 October 11

## ABSTRACT

We present an analysis of the effects of environment on the photometric properties of galaxies in the core of the Shapley Supercluster at  $z = 0.05$ , one of the most massive structures in the local universe. The Shapley Optical Survey (SOS) comprises archive WFI optical imaging of a  $2.0\text{ deg}^2$  region containing the rich clusters A3556, A3558 and A3562 which demonstrate a highly complex dynamical situation including ongoing cluster mergers. The  $B - R/R$  colour-magnitude relation has an intrinsic dispersion of  $0.045\text{ mag}$  and is  $0.015 \pm 0.005\text{ mag}$  redder in the highest-density regions, indicative of the red sequence galaxy population being 500 Myr older in the cluster cores than towards the virial radius. The  $B - R$  colours of galaxies are dependent on their environment, whereas their luminosities are independent of the local density, except for the very brightest galaxies ( $M_R < -22$ ). The global colours of faint ( $\gtrsim M^* + 2$ ) galaxies change from the cluster cores where  $\sim 90\%$  of galaxies lie along the cluster red sequence to the virial radius, where the fraction has dropped to just  $\sim 20\%$ . This suggests that processes related to the supercluster environment are responsible for transforming faint galaxies, rather than galaxy merging, which should be infrequent in any of the regions studied here. The largest concentrations of faint blue galaxies are found *between* the clusters, coincident with regions containing high fractions of  $\sim L^*$  galaxies with radio emission indicating starbursts. Their location suggests star-formation triggered by cluster mergers, in particular the merger of A3562 and the poor cluster SC 1329-313, although they may also represent recent arrivals in the supercluster core complex. The effect of the A3562-SC 1329-313 merger is also apparent as a displacement in the spatial distribution of the faint galaxy population from both the centres of X-ray emission and the brightest cluster galaxies for both systems. The cores of each of the clusters/groups are marked by regions that have the lowest blue galaxy fractions and reddest mean galaxy colours over the whole supercluster region, confirming that star-formation rates are lowest in the cluster cores. In the cases of A3562 and SC 1329-313, these regions coincide with the centres of X-ray emission rather than the peaks in the local surface density, indicating that ram-pressure stripping may have an important role in terminating any remnant star-formation in galaxies that encounter the dense ICM of the cluster cores.

**Key words:** Galaxies: clusters: general — Galaxies: clusters: individual: Shapley supercluster — Galaxies: photometry — Galaxies: evolution

## 1 INTRODUCTION

The cluster galaxy population has evolved rapidly over the last 4 Gyr (e.g., Butcher & Oemler 1978, 1984; Dressler et al. 1994, 1997; Treu et al. 2003; Kodama et al.

2004). Clusters at  $z \gtrsim 0.4$  are dominated, particularly at faint magnitudes, by blue spiral galaxies, predominantly irregular or Sc-Sd spirals. Some of these show signs of disturbed morphologies, and many present spectroscopic evidence that they have undergone multiple star-formation events over the last 1–2 Gyr (Dressler et al. 1994). Conversely, local clusters are completely dominated by passive

<sup>\*</sup> Based on European Southern Observatory archive data

<sup>\*\*</sup> E-mail:chris@na.astro.it

early-type galaxies: elliptical and lenticular (S0) galaxies at the brighter end, and dwarf spheroids at fainter magnitudes.

In the standard hierarchical cosmological model,  $z \sim 0.4$  represents the peak infall rate of field galaxies onto the cluster (Kauffmann 1995), and it is the transformation of these infalling field galaxies from star-forming disk-dominated galaxies into passively-evolving spheroids over a period of 4–5 Gyr through their encounter with the cluster environment, that produces the observed changes in cluster galaxy populations. Several physical mechanisms related to the cluster environment have been proposed as producing the observed transformations in galaxies, in which interactions with either other cluster galaxies or the hot intra-cluster medium (ICM) affect both their structural and star-formation properties.

To distinguish between these mechanisms it is necessary to examine both where the transformations occur, and how the star-formation and structural properties of the galaxies are changed (e.g. Treu et al. 2003). For example, ram pressure from the passage of the galaxy through the dense ICM can effectively remove the cold gas supply and thus rapidly terminate new star-formation, either by stripping the gas directly (Abadi, Moore & Bower 1999), or by inducing a starburst in which all of the gas is consumed (Fujita & Nagashima 1999). The most dramatic ICM-galaxy interactions should occur when two clusters merge, as shock fronts created in the ICM may trigger starbursts in galaxies over large scales (Roettiger, Burns & Loken 1996). Importantly, in terms of their environmental effects, these mechanisms all require a dense ICM, and so their evolutionary effects are limited to the cores of clusters.

In contrast, galaxy mergers, which can strongly affect the morphological evolution of disks, cannot occur when the encounter velocities are much greater than the internal velocity dispersion of galaxies (Aarseth & Fall 1980), and so while frequent in small groups, are rare in rich clusters (Ghigna et al. 1998). Alternatively galaxy harassment, whereby repeated close ( $< 50$  kpc), high-velocity ( $> 1000$  km s $^{-1}$ ) encounters with massive galaxies and the cluster’s tidal field cause impulsive gravitational shocks that damage the fragile disk of late-type spirals (Moore et al. 1996), transforming them over a period of several Gyr. Galaxy harassment is effective throughout a cluster, including beyond the virial radius, but its effects should be greater for those clusters with higher velocity dispersions.

Finally, when a galaxy falls into a more massive halo, the diffuse gas in its halo is lost to the ICM, thus preventing further cooling and replenishment of the cold gas supply, “suffocating” the galaxy (e.g. Blanton et al. 2000; Diaferio et al. 2001). Star-formation in the galaxy then declines slowly as the remaining cold gas is used up (Larson, Tinsley & Caldwell 1980).

The large datasets provided by the 2dFGRS and SDSS have allowed the environmental effects on galaxy properties to be followed statistically over the full range of environments, from the sparse field to the dense cluster cores (e.g. Lewis et al. 2002; Gómez et al. 2003), at least for the brightest galaxies ( $M < M^* + 1$ ). They show that star-formation is most closely dependent on local density, and is systematically suppressed above a critical value of density, that is found 3–4 virial radii from clusters, but also in galaxy groups as poor as  $\sigma \sim 100$  km s $^{-1}$ . This suppression is ob-

served to be independent of the richness of the structure to which the galaxy is bound (Tanaka et al. 2004), indicating that mechanisms such as galaxy harassment or ram-pressure stripping are not important for the evolution of bright galaxies. Instead the strongest candidates for driving their transformation are galaxy suffocation and low-velocity encounters, which are effective in both galaxy groups and cluster infall regions.

However, it is not clear if and how this scenario extends to fainter magnitudes, as there has been observed a strong bimodality in the properties of galaxies about a characteristic stellar mass  $\sim 3 \times 10^{10} M_{\odot}$  (corresponding to  $\sim M^* + 1$ ), with more massive galaxies predominately passive red spheroids, and less massive galaxies tending to be blue star-forming disks (Kauffmann et al. 2003). This bimodality implies fundamental differences in the formation and evolution of giant and dwarf galaxies, and it has been proposed (e.g. Dekel & Birnboim 2006; Kereš et al. 2005) that these are driven by thermal processes in the gas inflowing from the halo onto the galaxy, with the characteristic mass scale representing the point at which shocks in the halo become stable, heating up the halo gas, and preventing further cooling. Hence if the formation and evolution of giant and dwarf galaxies are so fundamentally different, then they are likely to be affected differently by mechanisms related to the environment. For example, galaxy harassment should be most efficient at transforming low-luminosity late-type galaxies. Tanaka et al. (2004) find differences in the environmental dependences of faint ( $M^* + 1 < M < M^* + 2$ ) and bright ( $M < M^* + 1$ ) galaxy populations, and suggest that faint galaxies are affected by mechanisms related to the structure in which the galaxy is found.

To understand the mechanisms underlying the transformation of faint galaxies requires datasets reaching much fainter luminosities. Crucial discriminators between the different transformation mechanisms are the time- and distance-scales involved: while ram-pressure stripping should rapidly terminate star-formation in a galaxy within  $\lesssim 100$  Myr but requires the dense ICM of the cluster core; a galaxy undergoing suffocation will have its star-formation rate slowly decline over a period of several Gyr. Hence the nature of the transition from regions where the majority of galaxies are star-forming, and those dominated by passive galaxies, will depend strongly on the dominant mechanism involved.

One approach is to use galaxy colours, which can be readily obtained to much fainter magnitudes than spectroscopic star-formation rates, and which through the use of models can be directly related to star-formation histories with minimal assumptions (e.g. Bruzual & Charlot 2003). Recent large datasets have shown that the bimodality of galaxies is also manifested through their broadband photometry, in particular a separation can be made on the basis of colour into red and blue galaxy populations (Strateva et al. 2001; Blanton et al. 2003), which correspond roughly to the two broad types previously known from their morphological and spectroscopical characteristics: passively-evolving early-type and star-forming late-type galaxies. This bimodality has been further quantified, resulting in colour-magnitude (C-M) relations and for both the red and blue galaxy populations (Baldry et al. 2004), and its evolution observed to  $z \sim 1$  (Bell et al. 2004). Balogh et al. (2004) show that the

bimodal galaxy colour distribution is strongly dependent on environment, with the fraction of galaxies in the red distribution at a fixed luminosity increasing from 10–30% in the lowest density environments, to  $\sim 70\%$  at the highest densities.

The most dramatic effects of environment on galaxy evolution should occur in superclusters, where the infall and encounter velocities of galaxies are greatest ( $>1000 \text{ km s}^{-1}$ ), groups and clusters are still merging, and significant numbers of galaxies will be encountering the dense ICM of the cluster environment for the first time.

With this in mind we are undertaking the Shapley Optical Survey (SOS), an optical photometric study of the core region of the Shapley supercluster (Shapley 1930), one of the most massive structure in the local universe, containing as many as 25 Abell clusters.

In this paper we examine the effect of the supercluster environment on the star-formation histories of galaxies as measured through their galaxy colours. We present the SOS in Section 2, and then describe how we quantify the local environment and statistically subtract the field galaxy population in Sections 3 and 4. We present our analysis of the C-M relation in Section 5, which then allows us to separate the red and blue galaxy populations whose spatial distributions are presented in Section 6. We examine the environmental dependencies on galaxy colours in Section 7, and discuss our findings in Section 8, before presenting our conclusions in Section 9. Throughout the paper we adopt a cosmology with  $\Omega_M = 0.3$ ,  $\Omega_\Lambda = 0.7$  and  $H_0 = 70 \text{ km s}^{-1} \text{ Mpc}^{-1}$ . According to this cosmology 1 arcmin corresponds to 60 kpc at  $z = 0.048$ .

## 2 THE SHAPLEY OPTICAL SURVEY

The SOS comprises wide-field optical imaging of a  $2.0 \text{ deg}^2$  region covering the whole of the Shapley supercluster core (hereafter SSC), which comprises three Abell clusters A3556, A3558 and A3562 and two poor clusters SC 1327–312 and SC 1329–314. The resultant galaxy catalogues are complete to  $R = 22.0$  and  $B = 22.5$ , allowing us for the first time to study the effect of the supercluster environment on the photometric properties of galaxies, particularly the dwarf galaxy population where we reach  $M^* + 7$ .

The area is covered by extensive redshift surveys (e.g. Bardelli et al. 2000; Quintana, Carrasco & Reisenegger 2000; Drinkwater et al. 2004) which indicate that these clusters form a complex clumpy and highly-elongated structure  $\sim 9 h_{70}^{-1} \text{ Mpc}$  across, which is in the final stages of collapse, with infall velocities reaching  $2000 \text{ km s}^{-1}$  (Reisenegger et al. 2000). There exists a wealth of multi-wavelength data from radio (e.g. Miller 2005) to X-ray (e.g. Finoguenov et al. 2004), which in conjunction with the redshift data, describe a dramatic scenario with ongoing cluster-cluster mergers triggering star-formation in galaxies over  $\sim \text{Mpc}$  scales. It is clear that amid this maelstrom of galaxies, groups and clusters, both galaxy harassment and ram pressure stripping should be at their most effective in transforming the infalling field galaxies.

We aim to use the SOS dataset to study the effect of environment on the luminosity distribution, colours and structural properties of galaxies, and through comparison with

numerical simulations and theoretical predictions, draw insights regarding which physical processes are most important for the transformation and evolution of galaxies in these environments.

In Mercurio et al. (2006, hereafter Paper I) we introduce the survey, and describe the observations, calibrations, and derivation of the galaxy catalogues. The galaxy luminosity functions are also presented, and significant environmental effects are observed, in the form of a dip at  $\sim M^* + 2$  which becomes deeper, and a faint-end slope which becomes steeper, with decreasing density. We explain these results in terms of the galaxy harassment scenario, in which the late-type spirals that represent the dominant population at  $\sim M^* + 2$  are transformed by galaxy harassment into passively-evolving dwarf spheroids, and in the process become  $\sim 1\text{--}2$  magnitudes fainter due to mass loss and an ageing stellar population without new star-formation.

In this paper we examine the effect of the supercluster environment on the star-formation histories of galaxies as measured through their galaxy colours, while in future papers we expect to consider the environmental impact on galaxy structural parameters and compare our observational results with semi-analytical models of galaxy evolution in n-body simulations of a supercluster region.

The data were obtained from the ESO science archive (68.A-0084, P.I. Slezak), comprising wide-field  $B$ - and  $R$ -band imaging covering a  $2.0 \text{ deg}^2$  region towards the clusters A3562, A3558 and A3556 which form the core of the Shapley supercluster at  $z \sim 0.05$ . Full details of the observations, data reduction, and the production of the galaxy catalogues are described in Paper I, and only a summary is presented below.

The observations were made from March 2002 to April 2003 using the WFI camera, an instrument made up of eight  $2046 \times 2048$  CCDs giving a field of view of  $34' \times 33'$ , and which is set at the Cassegrain focus of the 2.2-m MPG/ESO telescope at La Silla. The survey is made up of eight contiguous fields, each with total exposure times of 1500 s in  $B$  and 1200 s in  $R$ , and typical FWHMs of  $0.7\text{--}1.0''$ . The data are reduced using the ALAMBIC pipeline (version 1.0, Vandame 2004), and calibrated to the Johnson-Kron-Cousins photometric system using observations of Landolt (1992) standard stars. The sources are then extracted and classified using SExtractor (Bertin & Arnouts 1996), resulting in galaxy catalogues which are both complete and reliable (i.e. free of stars) to  $R = 22.0$  and  $B = 22.5$ . For this analysis we consider only galaxies to  $R = 21.0$  where uncertainties in the photometry are less than 0.1 mag in both  $R$  and  $B - R$  for galaxies belonging to the supercluster.

## 3 QUANTIFYING THE GALAXY ENVIRONMENT

To study the effect of the cluster environment on galaxies in the SSC, the local density of galaxies,  $\Sigma$ , is determined across the SOS mosaic. This is achieved using an adaptive kernel estimator (Pisani 1993, 1996), in which each galaxy  $i$  is represented by a Gaussian kernel,  $K(r_i) \propto \exp(-r^2/2\sigma_i^2)$ , whose width,  $\sigma_i$  is proportional to  $\Sigma_i^{-1/2}$  thus matching the resolution locally to the density of information available. For this study, we consider the surface number density of

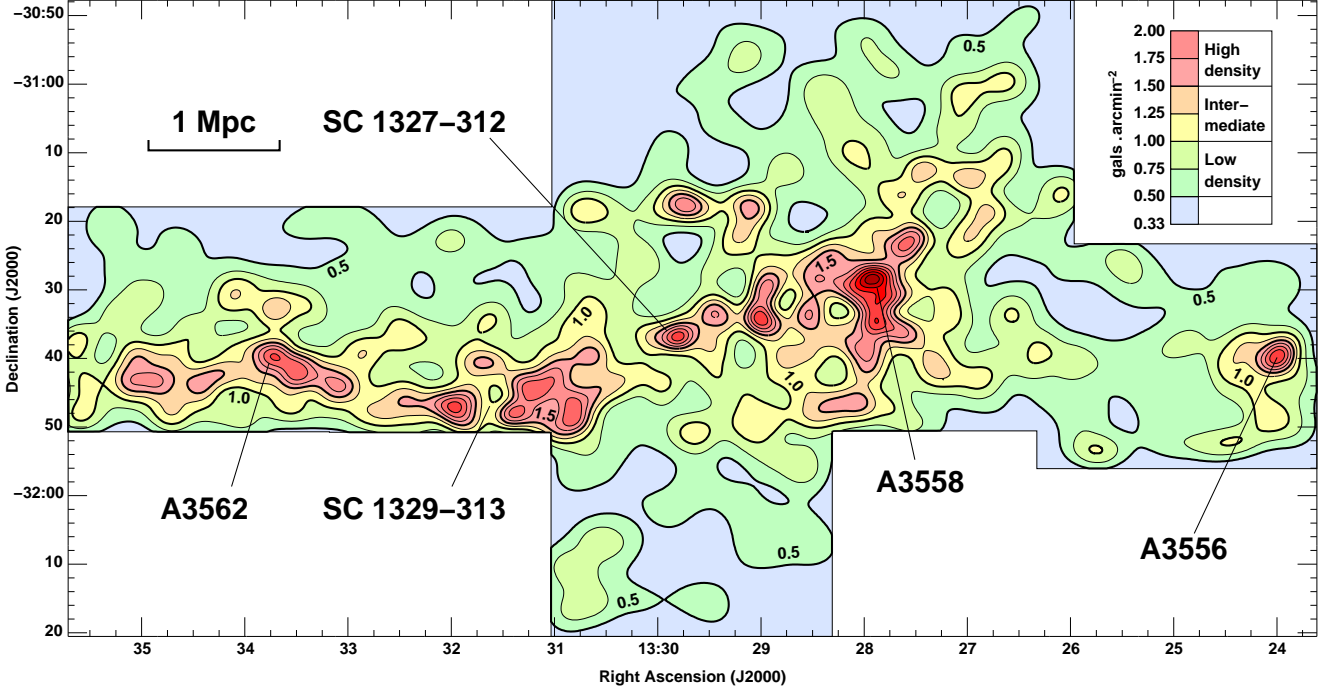


**Figure 1.** The surface density of  $R < 21.0$  galaxies in the region of the Shapley Supercluster core complex. Isodensity contours are shown at intervals of  $0.25 \text{ gals arcmin}^{-2}$ , with the thick contours corresponding to  $0.5$ ,  $1.0$  and  $1.5 \text{ gals arcmin}^{-2}$ , the densities used to separate the three cluster environments. High-density regions ( $\Sigma > 1.5$ ) are indicated by red colours, while intermediate- ( $1.0 < \Sigma < 1.5$ ) and low-density ( $0.5 < \Sigma < 1.0$ ) regions are indicated by yellow/orange and green colours respectively. The centres of X-ray emission for each of the clusters are indicated.

$R < 21.0$  ( $< M^* + 6$ ) galaxies, with an additional colour cut applied to reject those galaxies more than  $0.2 \text{ mag}$  redder in  $B - R$  than the observed cluster red sequence to minimize background contamination. As there are no known structures in the foreground of the SSC (90% of  $R < 16$  galaxies have redshifts confirming that they belong to the supercluster), any substructure identified in the density map is likely to be real and belonging to the supercluster. The local density is initially determined using a fixed Gaussian kernel of width  $2 \text{ arcmin}$ , and then iteratively recalculated using adaptive kernels. The resultant surface density map of the SSC is shown in Fig 1, with the three clusters and two groups indicated. Isodensity contours are shown at intervals of  $0.25 \text{ gals arcmin}^{-2}$ , with the thick contours corresponding to  $0.5$ ,  $1.0$  and  $1.5 \text{ gals arcmin}^{-2}$ , the densities used to separate the three cluster environments described below.

The expected density of field galaxies is estimated through analysis of thirteen  $35' \times 35'$  fields of deep  $BVR$  imaging taken from the Deep Lens Survey (DLS; Wittman et al. 2002). These data covering  $4.3 \text{ deg}^2$  in total, were taken using the Mosaic-II cameras on the NOAO KPNO and CTIO 4-m telescopes, and have  $5\sigma$  depths of  $B, V, R \sim 27$  and typical  $R$ -band FWHMs of  $0.9''$ , allowing accurate photometric measurements and star-galaxy classifications to be made to at least the depths of our survey. Through applying the same colour-magnitude cuts, we estimate the density of field galaxies to be  $0.335 \pm 0.019 \text{ gals arcmin}^{-2}$ , and hence the thick contours correspond to overdensity levels of  $\sim 50$ ,  $200$  and  $400 \text{ gals } h_{70}^2 \text{ Mpc}^{-2}$  respectively. The entire region covered

by the SOS can be seen to be overdense with respect to field galaxy counts.

For the following analyses on the effect of the cluster environment on its constituent galaxy population we define three regions selected according to the local surface number density. Firstly we consider a high-density region with  $\Sigma > 1.5 \text{ gals arcmin}^{-2}$  which correspond to the cores of the clusters. Next we consider intermediate- ( $1.0 < \Sigma < 1.5$ ) and low-density ( $0.5 < \Sigma < 1.0$ ) regions which probe the filament connecting the clusters A3562 and A3558, as well as the wider envelope containing the whole supercluster core complex.

#### 4 STATISTICAL FIELD GALAXY SUBTRACTION

To accurately measure the global photometric properties of the galaxy population in the SSC requires the foreground / background contamination to be estimated efficiently and corrected for. There exists already a wealth of spectroscopic data in the region, comprising 607 published galaxy redshifts (Bardelli et al. 1998) corresponding to 90% of  $R < 16$  galaxies, dropping to 50% for  $R < 17.7$ . For those galaxies without redshifts, particularly at fainter magnitudes, we estimate the probability that they are supercluster members. This probability is dependent on the spatial position, the  $R$ -band magnitude and  $B - R$  colour. The dependence on its spatial position, through its local number density, is clear as galaxies towards one of the density peaks will be more

likely to be members than those in regions where the surface density is closer to that expected for the field. The dependence on the galaxies colour and magnitude is complex, with galaxies located on the cluster red sequence most likely to be members, while those galaxies much redder than the sequence most likely to belong to the background population. It is important that all three parameters are considered simultaneously, as the relationship between the broad-band properties of galaxies and their environment has been shown to be complex (Blanton et al. 2003).

We account for this by considering separately the three cluster environments described previously when estimating the probability that galaxies are supercluster members through their  $R$ -band magnitude and  $B - R$  colour using the methods described in Kodama & Bower (2001). For each of these three cluster environments and the Deep Lens Survey field comparison, two-dimensional histograms are built with bins of width 0.4 mag in  $R$  and 0.2 mag in  $B - R$  to properly map the galaxy C-M distribution. The histogram of field galaxies is normalised to match the area within each cluster region, and for each galaxy, the probability that galaxy  $i$  belongs to the supercluster is then defined as:

$$P_{SC}^i = \frac{\Sigma_{SC}(R, B - R)_i - \Sigma_{field}(R, B - R)_i}{\Sigma_{SC}(R, B - R)_i}, \quad (1)$$

where  $\Sigma_{SC}(R, B - R)_i$  and  $\Sigma_{field}(R, B - R)_i$  are the number densities of galaxies in the supercluster and field environments belonging to the corresponding bin in  $R$  and  $B - R$ . In low-density environments it is possible that  $\Sigma_{SC}(R, B - R)_i < \Sigma_{field}(R, B - R)_i$  for a particular bin, and so in these cases the excess number of field galaxies are redistributed to neighbouring bins with equal weight until  $\Sigma_{SC}(R, B - R)_i \geq \Sigma_{field}(R, B - R)_i$  for all bins. For those galaxies with redshifts  $P_{SC}^i$  is set to 1 for  $0.035 < z < 0.056$  (the redshift range of known supercluster members in the SOS field) or 0 otherwise. Hence for each  $R < 21$  galaxy in the region covered by the SOS, we estimate the likelihood of its belonging to the Shapley supercluster based upon its  $R$ -band magnitude,  $B - R$  colour and local density.

## 5 THE COLOUR-MAGNITUDE RELATION

To estimate the location of the colour-magnitude relation for galaxies in the supercluster, we consider those galaxies with local densities  $\Sigma > 1.0$ , i.e. both intermediate- and high-density environments, in order to avoid *a priori* field contamination effects when measuring the C-M slope. Figure 2 shows the resulting C-M diagram for a Monte Carlo realisation of the galaxy population in these regions, in which those galaxies predicted to belong to the supercluster indicated by the larger symbols, and those belonging to the field indicated by the small points. A clear red sequence is apparent for  $13 < R < 20$ . However at  $R < 15$  it becomes notably flatter, while at  $R > 19$  it becomes increasingly difficult to separate it from the remainder of the cluster population. This flattening at the brightest magnitudes has been noted previously for this region (Metcalfe et al. 1994), and has been observed for a large sample of galaxies from the Sloan Digital Sky Survey (Baldry et al. 2004), indicating this is a universal phenomenon. The slope in the C-M relation has been considered due to a progressive increase in metallicity with mass

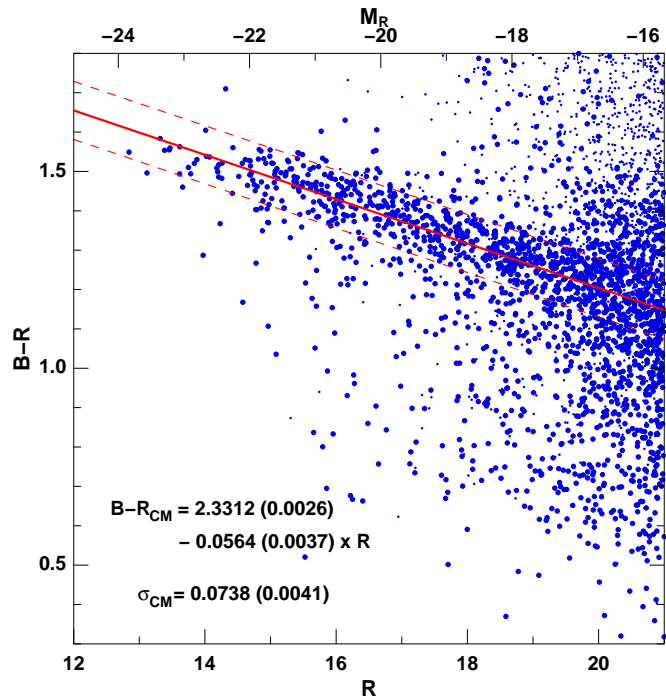


**Figure 2.** The  $B - R/R$  colour-magnitude diagram of galaxies in the regions corresponding to intermediate- and high-densities ( $\Sigma > 1.0 \text{ gal arcmin}^{-2}$ ). The larger points represent a Monte Carlo realisation of the supercluster galaxy population, while the remaining (and hence field) galaxies are shown by the small points. The best-fitting C-M relation is indicated by the solid red line, with the parallel dashed lines indicating the  $1\sigma$  dispersion levels.

due to the greater ability of more massive galaxies to retain metals dispersed by supernova during their formation, and so the observed flattening of the C-M slope probably represents the same flattening of the mass-metallicity seen for galaxies with  $M_* \gtrsim 10^{10.5} M_\odot$  (Tremonti et al. 2004), which in turn may reflect the observation that the brightest galaxies are built up through “dry mergers” of  $\sim M^*$  galaxies (e.g. Faber et al. 2005), and hence would have the same metallicities and colours as their progenitors.

We perform a fit to the C-M relation over the range  $14.5 < R < 19.0$ , where the red sequence relation appears linear and can be separated from the rest of the cluster population. Although the red sequence appears visually quite distinct, obtaining a robust fit to it is not trivial, particularly given the presence of outliers which are heavily skewed bluewards of the relation, and so simple least-squares methods are unsuitable. We apply the same method as López-Cruz et al. (2004), which produced the most robust results by iteratively applying the biweight algorithm (Beers, Flynn & Gebhardt 1990) with  $3\sigma$  clipping to counteract the heavily skewed distribution. A range of slope values were searched to determine the best-fitting value that minimizes the biweight scale of the deviations from the median value.

The uncertainties in the slope and intercept are derived using the non-parametric bootstrap method. The number of cluster galaxies,  $n$ , is estimated as  $n = \sum_{i=1}^N P_{SC}^i$  for the  $N$  galaxies with  $14.5 < R < 19$ , and each bootstrap performed

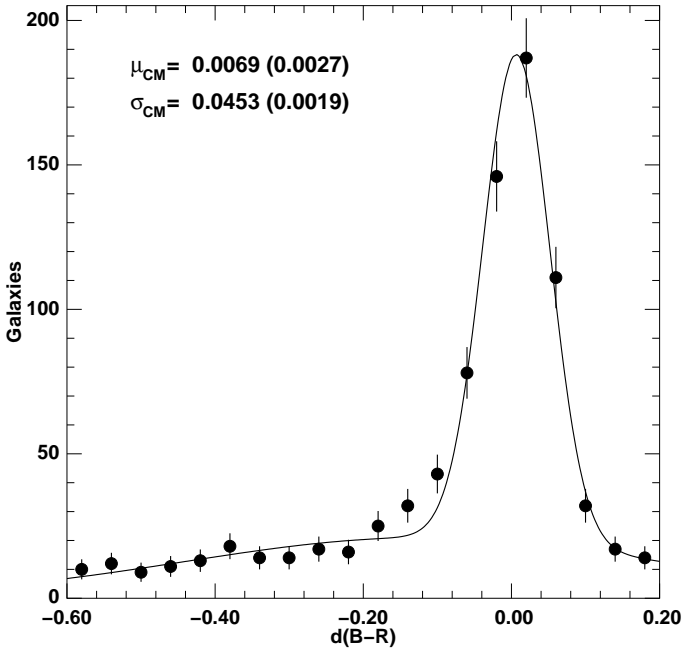


**Figure 3.** The distribution of  $B - R$  galaxy colours offsets from the C-M relation predicted by the biweight algorithm for  $R < 19$  galaxies with local densities greater than  $1.0 \text{ gal arcmin}^{-2}$ .

by sampling  $n$  galaxies with replacement according to the probabilities  $P_{SC}^i$  calculated using Eq. 1. Babu & Singh (1983) have analytically estimated that  $\sim n \log^2 n$  bootstrap resamplings give a good approximation to the underlying density population. The resultant best-fitting C-M relation is found to be:

$$(B - R)_{CM} = 2.3312 \pm 0.0026 - 0.0564 \pm 0.0037 \times R, \quad (2)$$

where the quoted uncertainty in the intercept assumes a fixed value of slope. The obtained dispersion about the relation as given by the biweight scale of the deviations is  $0.0738 \pm 0.0041 \text{ mag}$ .

As a robust test of the results obtained using the biweight algorithm, we plot a histogram of the distribution of  $\Delta(B - R)_{CM}$ , the  $B - R$  galaxy colour offset from the C-M relation, and model the distribution as a sum of two Gaussian functions, one to represent the red sequence, and another to represent the “blue cloud” population. Fig 3 shows that a bimodal Gaussian distribution describes well the distribution of  $\Delta(B - R)_{CM}$  ( $\chi^2/\nu \approx 1$ ), but with a mean offset of  $0.0069 \pm 0.0027 \text{ mag}$  with respect to the biweight median, and a dispersion of  $0.0453 \pm 0.0019 \text{ mag}$  that is significantly smaller than predicted by the biweight scale estimator, and comparable to the  $0.054 \text{ mag}$  dispersion observed for the Coma cluster in the same passbands (López-Cruz et al. 2004). Hence despite iteratively clipping galaxies  $> 3\sigma$  from the median value of the relation, both the intercept and dispersion of the relation obtained using the biweight algorithm have been affected by outliers and the heavily skewed distribution.

We do not expect that photometric uncertainties are a major contributor to the observed dispersion as: firstly the mean  $B - R$  uncertainty for galaxies in the red sequence is found to be  $0.012 \text{ mag}$ , only reaching  $0.025 \text{ mag}$  by  $R = 19.0$ ;

| $R < 21$ gals<br>$\text{arcmin}^{-2}$ | $\mu_{CM}$           | $\sigma_{CM}$       | $\frac{\chi^2}{\nu}$ |
|---------------------------------------|----------------------|---------------------|----------------------|
| $\Sigma > 1.0$                        | $+0.0069 \pm 0.0027$ | $0.0453 \pm 0.0019$ | 0.99                 |
| $\Sigma > 2.0$                        | $+0.0191 \pm 0.0064$ | $0.0460 \pm 0.0044$ | 0.24                 |
| $\Sigma > 1.5$                        | $+0.0142 \pm 0.0043$ | $0.0486 \pm 0.0031$ | 0.47                 |
| $1.0 < \Sigma < 1.5$                  | $-0.0004 \pm 0.0035$ | $0.0442 \pm 0.0024$ | 1.40                 |
| $0.5 < \Sigma < 1.0$                  | $-0.0012 \pm 0.0042$ | $0.0540 \pm 0.0031$ | 1.04                 |

**Table 1.** Gaussian fits to the  $B - R$  colour distribution around the C-M relation for  $R < 19$  galaxies in the different density environments

and secondly the observed dispersion does not vary significantly as a function of magnitude over  $14.5 < R < 19$ .

It is remarkable that such a small dispersion is obtained, given the large number of galaxies involved ( $\sim 600$ ) over two orders of magnitude in luminosity, and spread across three rich clusters and  $\sim 9 h_{70} \text{ Mpc}$ . The wide spread of redshifts within the supercluster complex ( $0.035 < z < 0.056$ ) could introduce a significant component to the observed dispersion through the spread of k-corrections required for the red sequence galaxies, as the predicted change in the  $B - R$  k-correction of an elliptical galaxy from  $0.035$  to  $0.056$  is  $\sim 0.08 \text{ mag}$  (Poggianti 1997), as is the observed increase in  $B - R$  colour of red sequence galaxies (López-Cruz et al. 2004).

To measure the possible effect of k-corrections on the obtained colour dispersion of red sequence galaxies, we consider those red sequence galaxies with known redshifts. Although the redshift data is less than 50% complete beyond  $R = 17.7$ , the  $B - R$  colour dispersion of the red sequence galaxies with redshifts is consistent with that for the whole  $R < 19$  sample. After applying suitable k-corrections to each of the galaxies with known redshifts, and the colour dispersion about the red sequence is recalculated, found to be still consistent with that before the k-correction has been applied. Hence the observed internal dispersion of galaxy colours around the red sequence is not primarily the effect of different k-corrections over the redshift range of the supercluster. This can be explained by considering that the redshift distribution has a standard deviation of  $0.0036$  ( $\sim 1100 \text{ km s}^{-1}$ ), corresponding to an rms  $\sigma$  of  $\sim 0.014 \text{ mag}$  in  $B - R$ , significantly smaller than the observed  $\sigma_{CM}$ .

To examine the effect of environment on the colour of the C-M relation we fit bimodal Gaussian distributions to the  $\Delta(B - R)_{CM}$  distribution in the three environments as parametrised by the local  $R < 21$  galaxy density. The slope and zero-point are maintained fixed at the values indicated in Eq. 2, in order to measure the shifts in the overall  $B - R$  colour of the red sequence with environment. We do not make any attempt to determine the slope and intercept in the differing environments using the biweight algorithm, as the effect of the heavily skewed distribution on the determination of these values will be dependent on environment, due to the increasing blue galaxy fraction from high- to low-density regions. Hence the resulting fits would be biased by the changing blue galaxy population, and mask any inherent changes in the red sequence population with environment.

The results of the Gaussian fits to the red sequence population are shown in Table 1. In each case the galaxy colour distribution is well described by a double Gaussian function.

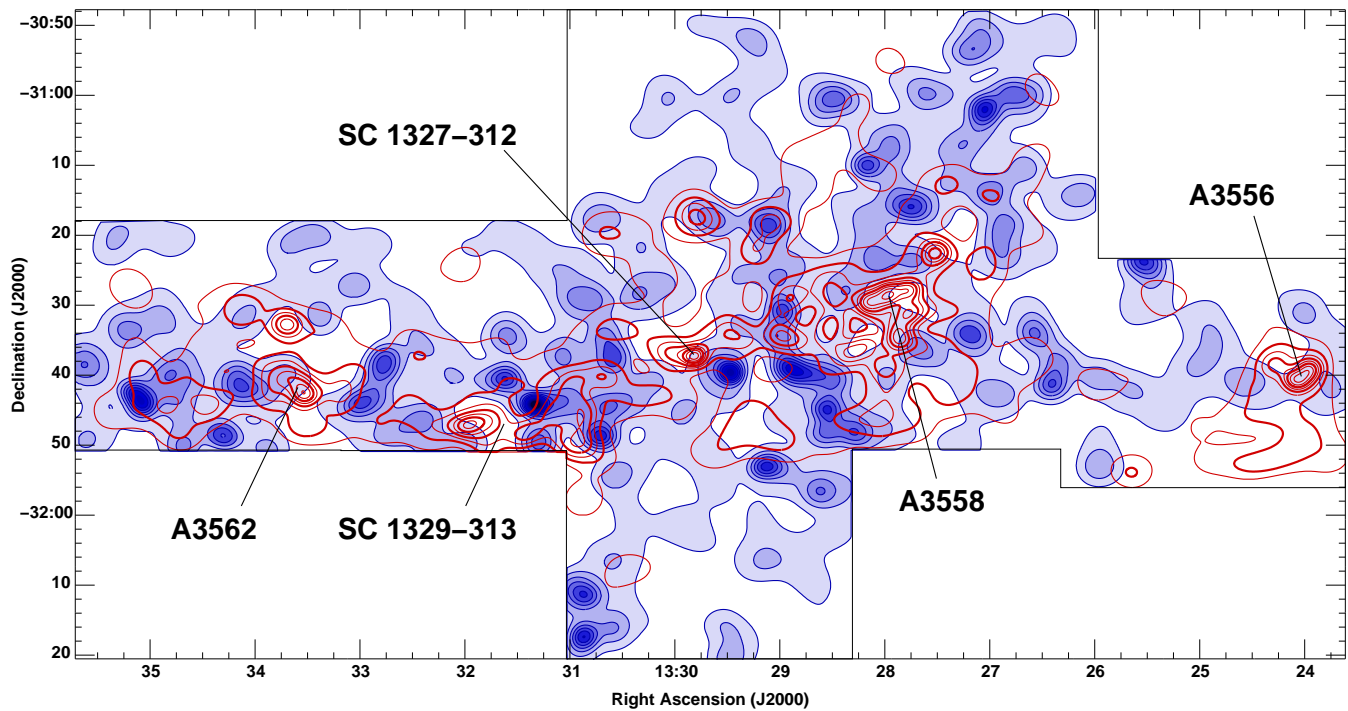


**Figure 4.** The surface density of  $R < 21$  galaxies  $> 3\sigma$  bluer than the cluster red sequence (blue filled contours) and those within  $3\sigma$  of the cluster red sequence (red contours) over the supercluster core complex. The isodensity contours for the blue galaxies are shown at intervals of  $0.125 \text{ gals arcmin}^{-2}$ , while the red contours are at intervals of  $0.25 \text{ gals arcmin}^{-2}$ . The centres of X-ray emission for each of the clusters are indicated.

The zero-points of the red sequence are consistent for the low- and intermediate-density regions, but the red sequence is found to be  $0.0147 \text{ mag}$  redder in the high-density region, a result significant at the  $2.6\sigma$  level. The redward shift of the red sequence continues if the density threshold is increased further, reaching  $0.0195 \text{ mag}$  for  $\Sigma > 2.0$ . The  $B - R$  colour dispersion of the red sequence remains constant at  $\sim 0.045$ , for each of the environments, suggesting that the observed reddening indicates an overall *shift* in the red galaxy population, rather than a *broadening* of the distribution due to increased numbers of bluer galaxies.

## 6 THE SPATIAL DISTRIBUTION OF RED AND BLUE GALAXIES

To examine where star-formation has been triggered or inhibited by the supercluster environment, we split the galaxy population into two according to colour. We identify red galaxies as those within  $3\sigma$  (after including photometric uncertainties) of the cluster red sequence, and blue galaxies as those  $> 3\sigma$  bluer than the red sequence. Hence these blue galaxies are all those *not* belonging to the red sequence, due to being either currently having some star-formation, or having had some in the previous  $\sim 2 \text{ Gyr}$ .

Figure 4 shows the spatial distribution of both red and blue galaxies over the supercluster complex, after correcting for the expected background contribution of  $0.147$  and  $0.071 \text{ gals arcmin}^{-2}$  for the red and blue galaxy subsets respectively, as estimated from the 13 Deep Lens Survey fields. The blue isodensity contours for the blue galaxies are shown at intervals of  $0.125 \text{ gals arcmin}^{-2}$ , which are filled with in-

creasingly intense blue colours with density. Overlaid are the red isodensity contours at intervals of  $0.25 \text{ gals arcmin}^{-2}$  to represent the local density of the red galaxy population. Note that all the contours indicate overdensities in comparison to the field, and that the spacing of the contours for the red galaxy population is twice that of the those for their blue counterparts. The centres of the X-ray emission from each of the clusters in the region are indicated.

The spatial distribution of the red and blue galaxy populations differ significantly. Whereas the blue galaxies appear reasonably evenly spread across the whole field, the red galaxies are highly concentrated towards the cluster centres and the filamentary structure connecting A3562 and A3558. In contrast, none of the three Abell or two poor clusters show particular overdensities in the blue galaxy distribution towards their cores, in fact they appear underdense in comparison to their immediate surroundings, as noted by Metcalfe et al. (1994) in the case of A3558. However, several localised overdensities of blue galaxies are apparent along the filamentary structure connecting A3562 and A3558, indicative of regions of enhanced star-formation within the supercluster core complex. What is particularly interesting is their distribution within the filamentary structure with respect to the clusters. The most overdense regions are located *between* each of the clusters A3562, A3558 and the two poor clusters. The two most notable overdensities of blue galaxies appear to be the western flank of the poor cluster SC 1329-313, and a linear structure bisecting the clusters A3558 and SC 1327-312. Both these overdensities contain numerous blue galaxies which are spectroscopically confirmed as belonging to the supercluster. The region where these overdensities of blue galaxies are located is where the two clus-

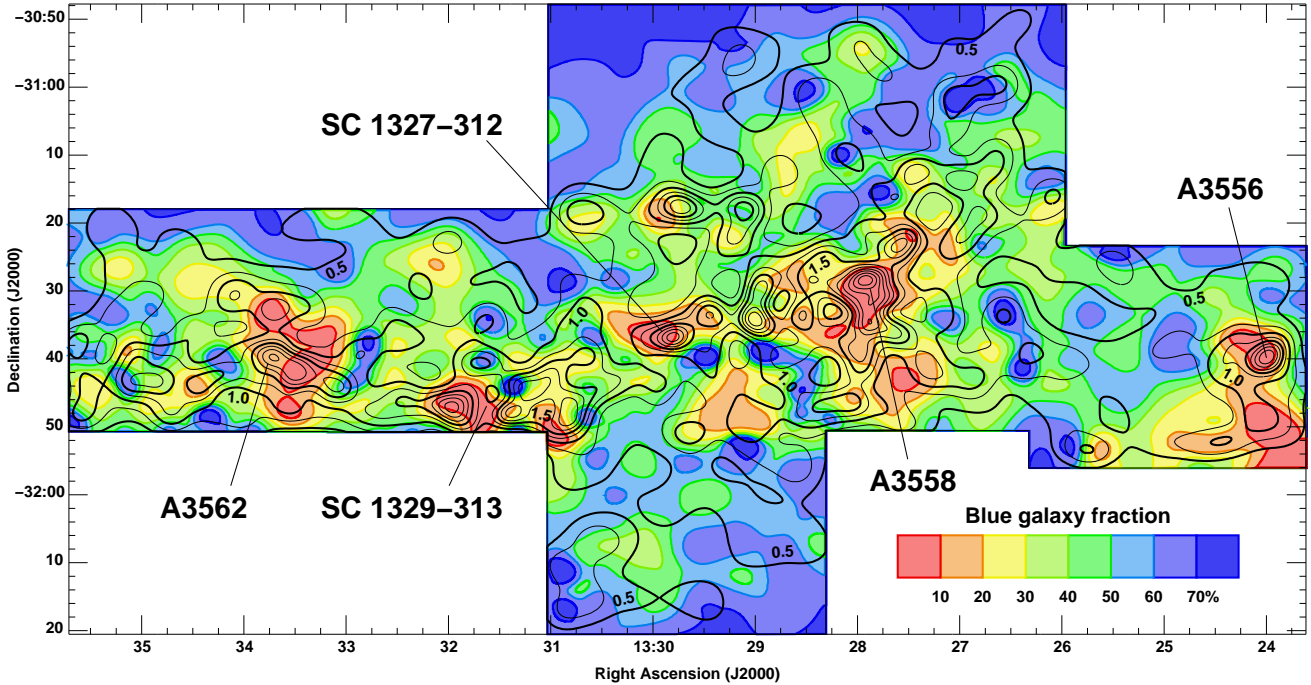


**Figure 5.** The fraction of  $R < 21$  galaxies  $> 3\sigma$  bluer than the cluster red sequence as a function of spatial position (see text).

ters A3562 and A3558 are both experiencing merging events, which may suggest that this merging has recently triggered star-formation in these blue galaxies, possibly through shock fronts produced when the ICMs of merging clusters collide. Alternatively these overdensities could reflect infall regions along the filament connecting the clusters A3558 and A3562.

Further insights into the effect of the supercluster on star-formation in its member galaxies are possible through the complementary information provided by the *fraction* of supercluster galaxies that are classed as blue. Figure 5 shows the fraction of  $R < 21$  galaxies  $> 3\sigma$  bluer than the cluster red sequence as a function of spatial position, as obtained by dividing the local surface density of blue galaxies by that for all  $R < 21$  galaxies after correcting both for background contamination. The blue galaxy fraction is represented by the coloured contours, with red indicating low blue galaxy fractions ( $< 10\%$ ) and blue indicating high blue galaxy fractions ( $> 50\%$ ). For comparison the isodensity contours of the overall  $R < 21$  galaxy density of Fig. 1 are overlaid.

Whereas the local blue galaxy density shows little correlation with that of the overall local galaxy density (see Fig. 4), the blue galaxy *fraction* appears strongly anti-correlated with the overall local galaxy density. Each of the three Abell clusters, and the two poor clusters, are marked by regions of low ( $< 10\%$ ) blue galaxy fractions, while the filamentary structure connecting the clusters A3562 and A3558 has typically  $\sim 20$ – $50\%$  blue galaxies, which rises still further for the regions furthest from the clusters. It is however this avoidance of the cluster cores by the blue galaxies that is the most notable feature of Fig. 5, with  $> 90\%$  of galaxies in these regions located within the narrow locus of the cluster red sequence to  $R = 21$  or  $M^* + 6$ . It is clear that in the central regions ( $r < 300$  kpc) of all the clusters

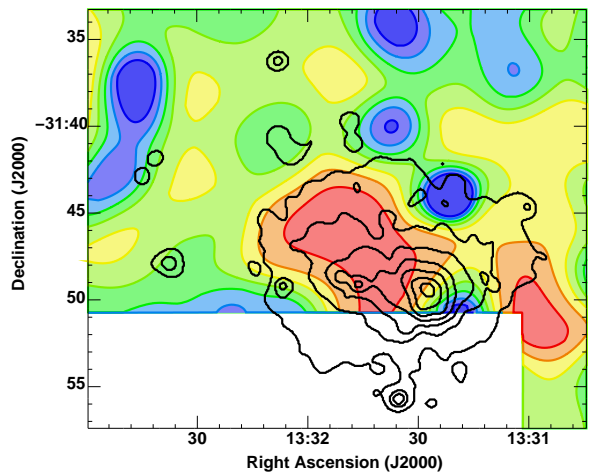


**Figure 6.** The relation between the fraction of blue galaxies (coloured filled contours as in Fig. 5) and X-ray emission (black contours) in the vicinity of the cluster SC 1329-313.

in this region star-formation has been severely truncated in *almost all if not all* galaxies.

A crucial insight into what physical process is resulting in this termination of star-formation can be obtained through comparison with complementary XMM X-ray imaging of the region around A3562 and SC 1329-313 as reported in Finoguenov et al. (2004). A comparison of their Fig. 1 shows that while the centre of the X-ray emission from A3562 is coincident with that obtained from our galaxy surface density, there is an extension to the north-east, where

we also find the blue galaxy fraction to be lowest as shown in Fig. 5.

Figure 6 shows how the blue galaxy fraction varies with spatial position in the vicinity of SC 1329-313, and whereas in Fig. 5 the overlaid black isodensity contours show the local galaxy density distribution, here they represent the X-ray emission from the ICM of SC 1329-313, taken from the XMM science archive (OID 10526, P.I. Aschenbach).

The centre of X-ray emission (as indicated by the arrow in Fig. 1) does not coincide well with either of the two peaks in the local galaxy density distribution, but appears to lie in between them. This displacement between the ICM and the galaxy distribution may be a dynamical effect from the merger, the result of the collisional gas lagging behind the collisionless DM and galaxies. A comparison of Figs. 4 and 6 suggests that while the region where the blue galaxy fraction is lowest does not coincide with either of the two peaks in the local galaxy distribution, it covers approximately the same region as the observed X-ray emission from the cluster. For both the clusters A3562 and SC 1329-313, regions where the blue galaxy fractions are lowest ( $< 20\%$ ) appear more strongly coincident with the centres and extensions of the X-ray emission, than the corresponding centres and extensions of the clusters as measured by the overall galaxy number density. The regions of low blue galaxy fractions appear coincident with the peaks in the galaxy surface density for the remaining clusters A3558, A3556 and SC 1327-312, and so it is not possible to separate the effects of galaxy density with those of the ICM for these regions.

## 7 THE RELATIONS BETWEEN COLOUR, LUMINOSITY AND ENVIRONMENT

As galaxy colours can be directly related to star-formation histories, by examining the environmental dependences of galaxy colours it is possible to gain insight into where and how star-formation is affected by the supercluster environment. Figure 7 shows the overall blue galaxy fraction as a function of local density for four different  $R$ -band magnitude ranges, quantifying the global anti-correlation with local density. The highest-density regions ( $\Sigma \gtrsim 1.5$ ) are dominated by red sequence galaxies over the entire magnitude range studied. There are two clear trends: the blue galaxy fraction decreases with increasing density; and in all environments the blue galaxy fraction increases monotonically with magnitude. The strength of this second trend appears greatest at  $R \sim 17$ : whereas at bright magnitudes ( $R < 17$  or  $M_R \lesssim M^* + 2$ ) the fraction of blue galaxies only increases marginally with decreasing local density, reaching only  $\sim 20\%$  at the lowest densities studied; at fainter magnitudes ( $R > 17$ ) the blue galaxy fraction increases rapidly to  $\sim 80\%$  in the lowest density bin.

The most luminous members of the supercluster are predominantly red sequence galaxies, and so would be expected to be strongly clustered in the high-density regions. To examine whether luminosity segregation contributes to the observed trends in galaxy colour with density, we plot in Fig. 8 the average environment as a function of both galaxy colour and magnitude. The grey-scale and contours indicate mean local density as a function of both the  $B - R$  colour offset and  $R$ -band magnitude, smoothed on scales

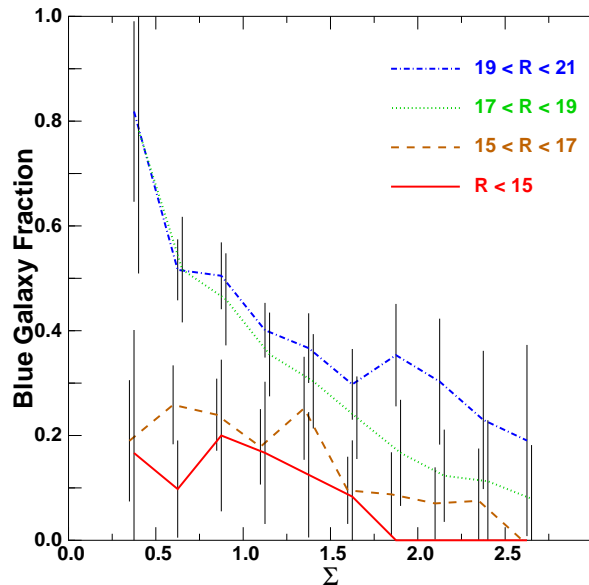


**Figure 7.** The blue galaxy fraction as a function of local density. Four lines are shown corresponding to four different  $R$ -band magnitude ranges as indicated.

of  $0.05$  mag in  $B - R$  and  $0.4$  mag in  $R$ . The global trends are very similar to those observed for galaxies in the SDSS (Blanton et al. 2004, 2005), with the predominantly horizontal contours indicating that for all but the brightest galaxies, where environment is strongly luminosity-dependent, local density is a strong function of galaxy colour, while remaining almost independent of luminosity. Red galaxies are typically found in high-density regions, while blue galaxies are on average located in low-density regions, the two populations separated at a density  $\sim 1.0$ – $1.1$  gals arcmin $^{-2}$ , or  $\sim 200$ – $250$  gals  $h_{70}^2$  Mpc $^{-2}$ . This separation reflects the trend shown in Fig. 7 for the blue galaxy fraction to increase with decreasing local density.

In a comparable study of the A901/902 supercluster at  $z = 0.16$ , Gray et al. (2004) use the 17-band COMBO-17 survey data to precisely isolate supercluster members within a thin photometric redshift slice ( $0.15 < z_{phot} < 0.18$ ). They find a strong segregation of faint quiescent and star-forming galaxies around a local surface density of  $\sim 200 h_{70}^2$  Mpc $^{-2}$  to a limit of  $M^* + 6$ , in excellent agreement with our value. While Gray et al. (2004) find a sharp transition in the galaxy properties at this density, our observed trends in mean galaxy colour and blue galaxy fractions with environment appear more gradual. This we put down to the fact that whereas Gray et al. (2004) use the 17-band photometry to accurately isolate the supercluster galaxies, we perform a statistical background subtraction based on just the  $R$ -band magnitude,  $B - R$  colour and local density, and hence any trends will be blurred out somewhat by interlopers.

We find that the brightest galaxies ( $R < 14$ ) are the most clustered, which could appear contrary to the results of Metcalfe et al. (1994) who found that  $b < 17$  galaxies within  $1.1$  Mpc of A3558 were significantly less clustered than those with  $b > 17$  both in projection and redshift space. However their limit of  $b = 17$  corresponds to  $R \sim 15.5$ , which is more

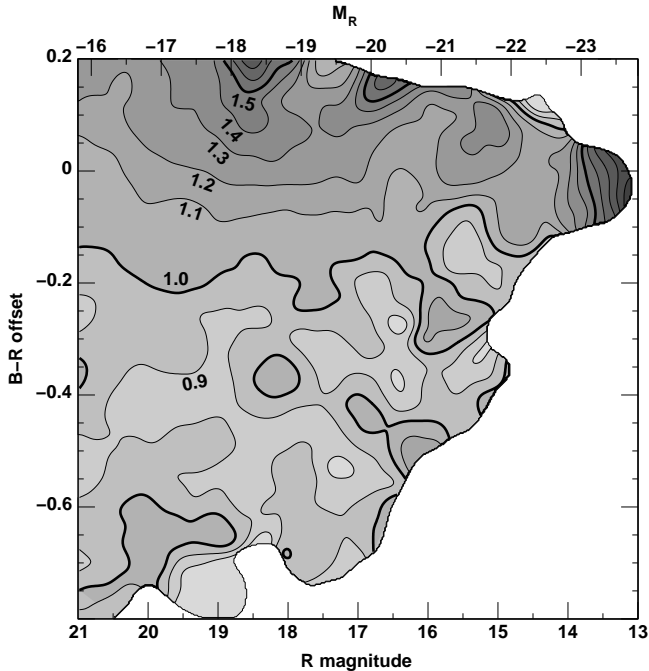


**Figure 8.** The mean local density as a function of the  $B - R$  colour offset from the red sequence and  $R$ -band magnitude.

than a magnitude fainter than the point at which we find luminosity segregation to become important.

Blanton et al. (2004) also reported that, as well the environments becoming denser with increasing luminosity for red galaxies at the brightest magnitudes, the environments of low-luminosity red galaxies become denser with increasing absolute magnitude down to  $M_R = -17.7$ , the limit of their survey. A similar phenomenon is apparent in our data, and although our survey extends two magnitudes fainter, we find that the trend for low-luminosity red galaxies to be found in dense environments is limited to those with  $M_R \sim -18$ . However it should be remembered that the uncertainties from the statistical background subtraction we have applied to measure the global supercluster galaxy populations become increasingly large at faint magnitudes.

## 8 DISCUSSION

We have examined the effect of the Shapley supercluster environment, as measured in terms of the local surface density of  $R < 21.0$  galaxies, on the star-formation histories of galaxies through their colours.

### 8.1 The Colour-Magnitude Relation

To examine the effect of environment on the *global* properties of red sequence galaxies, we measure the *overall* distribution of  $B - R$  colours with respect to the observed C-M relation using a double Gaussian fit to describe the global bimodal galaxy distribution. The use of this approach to measure environmental trends is vital, as the usual method of obtaining the best-fitting C-M relation and measuring the effect of environment on these fits are biased by the strongly skewed distribution and changing contribution of the blue galaxy pop-

ulation. We show that the *location* of the C-M relation is dependent on environment, with the relation  $0.0147 \pm 0.0055$  redder in  $B - R$  in the high-density regions corresponding to the cluster core ( $r \lesssim 0.3 h_{70}$  Mpc), than the low- and intermediate-density regions which represent the cluster periphery ( $0.3 \lesssim r \lesssim 1.5 h_{70}$  Mpc). This is a similar result to that obtained for the rich cluster A209 at  $z = 0.21$  where the red sequence was observed to be  $0.022 \pm 0.014$  mag redder in  $B - R$  in the cluster core than the periphery (Haines et al. 2004). By considering a model red sequence galaxy as a 10 Gyr old (at  $z = 0$ ),  $\tau = 0.01$  Gyr, solar-metallicity stellar population (Bruzual & Charlot 2003), the observed reddening of the C-M relation in the high-density region of A209 was interpreted as these galaxies being on average 500 Myr older or 20% more metal-rich than their counterparts in lower density environments. The observed reddening in the high-density regions of the Shapley supercluster is also consistent with the red sequence galaxies being  $\sim 500$  Myr older in the high-density regions than those in lower density environments, the resultant reddening of the  $B - R$  colour being 33% lower than for A209 as the galaxies should be on average 2 Gyr younger in A209 than in the Shapley supercluster.

These results are consistent with analysis of the spectra of 22 000 luminous, red, bulge-dominated galaxies from the SDSS, which were found to be marginally older and more metal-rich in high-density regions than their low-density counterparts (Eisenstein et al. 2003), although they were unable to quantify these differences due to their models being unable to vary  $\alpha$ -Fe abundance ratios. By considering the effects of age, metallicity and  $\alpha$ -Fe ratios simultaneously on the spectra of 124 local early-type galaxies, Thomas et al. (2005) show that those in high-density environments are  $\sim 2$  Gyr older and slightly (10–25%) more metal-rich than their counterparts in field regions. We should expect much smaller differences in the predicted average ages of red sequence galaxies as even our low-density environments are typically within 1 cluster radii, while gradients in the star-formation histories of cluster galaxy populations have been shown to extend out to 3–4 virial radii before reaching field values.

These results are understandable in the framework of cosmological structure formation models, in which galaxies form earliest in the highest-density regions corresponding to the cluster cores, and have their star-formation terminated earliest as the cores become filled with shock-heated virialised gas which does not easily cool or collapse, suppressing further formation of stars and galaxies (Blanton et al. 2000). Age-gradients remain in clusters to this epoch, as mixing of the galaxy population is incomplete, and the position of the galaxies within the cluster are correlated with the epoch at which they were accreted, and the point at which star-formation within them is suppressed (Diaferio et al. 2001).

### 8.2 Galaxy Colours

We identify two predominant trends relating galaxy colours, luminosities and their local environment: the anti-correlation between blue galaxy fraction and local density; and the monotonic increase in the blue galaxy fraction with  $R$ -band magnitude in all environments studied. These trends mirror those obtained by Balogh et al. (2004) relating the red galaxy fraction (selected by  $u - r$  colour),  $M_r$  and local

density for galaxies taken from the SDSS first data release, although they indicate that the strength of the trend with environment is independent of luminosity, whereas we find that the effect of environment on the blue galaxy fraction is much greater at fainter magnitudes ( $17 < R < 21$ ) than at brighter magnitudes ( $R < 17$ ) where red galaxies dominate in all environments. As all the environments studied here lie within  $\sim 1 R_{\text{vir}}$  of one of the clusters, this suggests that processes related to the supercluster environment are much more important for the evolution of faint galaxies ( $\gtrsim M^*+2$ ) than their brighter counterparts.

We find that the  $B - R$  colour of a galaxy is dependent its environment, whereas its luminosity is independent of local density, except at the very brightest magnitudes ( $M_R < -22$ ). Red galaxies located on average in regions with a mean local density greater than  $1.0\text{--}1.1 \text{ gals arcmin}^{-2}$  ( $\sim 200\text{--}250 h_{70}^2 \text{ Mpc}^{-2}$ ), while blue galaxies are on average found in less dense regions.

We find evidence for an increase in clustering of low-luminosity red galaxies as also observed in the SDSS (Blanton et al. 2004; Zehavi et al. 2005). The effect appears to be greatest at  $M_R \sim -18$ , with fainter red galaxies found in less dense environments. This is most likely to be related to the dramatic effects of environment on the luminosity function of faint galaxies observed for this region described in Paper I, in which dips are apparent at  $-18 \lesssim M_R \lesssim -20$ , which becomes deeper with decreasing local density. The observed dips are due to a relative lack of red sequence galaxies at these magnitudes in the lower density regions in comparison to the cluster core, and so it is manifested here as an enhanced clustering of red galaxies at  $M_R \sim -18$ . These observed changes in the galaxy luminosity function with environment were explained in Paper I in terms of the galaxy harassment scenario, in which infalling Sc-Sd spiral galaxies are transformed by repeated high-velocity encounters over a period of several Gyr, and in the process become 1–2 mag dimmer due to both mass loss and as a result of their star-formation being terminated (Moore, Lake & Katz 1998). These galaxies which predominate in  $z \sim 0.4$  clusters at  $M_R \sim -20$  are thus shifted to fainter magnitudes, producing the observed dip, and hence the red galaxies at  $M_R \sim -18$  are found preferentially in the highest-density environments as they are produced as a direct result of harassment by the supercluster environment. At fainter magnitudes the harassment becomes too great, and in fact the dwarf galaxies are completely disrupted by tidal forces in the cluster centre (Moore et al. 1998) and their stars cannibalised by the cD galaxy.

### 8.3 Galaxy colours and the ICM

The cores of each of the clusters are completely dominated by red sequence galaxies, as indicated by regions containing very low fractions ( $< 10\%$ ) of blue galaxies, and red mean galaxy colours. In the cases of A3562 and SC 1329-313 these regions, which coincide with both the centres of X-ray emission and the location of the brightest cluster galaxy (BCG), are displaced from the peaks in the  $R < 21$  galaxy surface density, particularly for SC 1329-313. The displacement, at least between the X-ray emission/BCG and the peaks in the galaxy surface density are likely to be related to the dynamics of the system, that is an ongoing cluster merger, which

has been proposed from an analysis of the X-ray emission (Finoguenov et al. 2004) and the finding of a young radio halo at the centre of A3562 (Venturi et al. 2000). The strong correlation between the regions devoid of blue galaxies and the X-ray emission, as opposed to the density peaks, may be evidence in support of ram pressure stripping having an important role in terminating any remnant star-formation in galaxies that encounter the cluster cores, although equally it could be a consequence of the dynamics of the system displacing the faint galaxy population.

The A3562–SC 1329-313 system appears the most active in terms of star-formation, with the highest densities of blue galaxies across the supercluster survey region found here, in particular the north-western flank of SC 1329-313, but also between the two clusters. These are also the regions where in a  $7 \text{ deg}^2$  VLA radio survey of the whole supercluster core complex Miller (2005) found dramatic increases in the fraction of  $\sim M^* + 1$  galaxies belonging to the supercluster (i.e. with redshifts) which have associated radio emission. From a visual inspection of their morphology, these radio emitters are found to be spirals/irregulars, and this region marks the greatest concentration of bright  $R < 16$  spiral galaxies across the supercluster complex. Miller (2005) interpreted these as young starburst galaxies related to the cluster merger event, and taking this in addition to our results which are sensitive to the dwarf galaxy population, we can say this star-formation activity extends to  $M^* + 6$ .

Are these galaxies which are undergoing starbursts triggered by the effects of the cluster merger, for example by encountering shocks in the ICM (Roettiger et al. 1996), or are they are a group of normal star-forming galaxies which have just entered the supercluster ?

Through an analysis of the X-ray emission from A3562 and SC 1329-313, Finoguenov et al. (2004) argued that SC 1329-313 had recently passed westwards through the northern outskirts of A3562 and then been deflected south. This would appear to contradict the idea that SC 1329-313 is a remnant from the ongoing A3562-A3558 merger, and instead suggests it represents a recent arrival in the supercluster core complex. However the regions containing the largest concentrations of faint blue galaxies are located *between* clusters, in particular along the filament connecting the clusters A3558 and A3562, which would support the hypothesis that shocks in the ICM produced by cluster mergers is triggering starbursts in these galaxies.

## 9 CONCLUSIONS

The area covered by the SOS dataset lies mostly within one virial radius ( $1\text{--}1.5 h_{70} \text{ Mpc}$ ) of one of the clusters. The results presented here and in Paper I show that the global properties of faint galaxies change significantly from the cluster cores to the virial radius, both in terms of the luminosity function, and the mean galaxy colours, which indicates that these galaxies are being transformed by processes related to the supercluster environment. As galaxy mergers should be infrequent in any of the environments covered by the SOS, the finding of such large changes in the mean galaxy colour or fraction of faint blue galaxies within the SOS, indicates that some process other than merging must be responsible. In paper I, we suggested that galaxy harass-

ment is important for shaping the galaxy luminosity function at magnitudes fainter than  $\sim M^* + 1$ , and here we find additional evidence in favour of faint galaxies being transformed by ram-pressure stripping and undergoing starbursts triggered by shocks in the ICM produced by cluster mergers.

These results indicate that the effect of environment on faint ( $\gtrsim M^* + 1$ ) galaxies is quite different from that observed for bright galaxies (Gómez et al. 2003; Lewis et al. 2002). While bright galaxies appear to be transformed by processes that can take place well outside the virial radius, that is galaxy merging or suffocation, we find here that many faint galaxies are affected by their interaction with the supercluster environment, although we cannot rule out that the faint galaxies are also transformed outside the virial radius, beyond the limits of our survey. It is also possible that the observed environmental trends are partly due to a population of primordial, early-type galaxies that formed preferentially in the high-density regions that later became clusters (e.g. Poggianti 2006). The differences in the environmental trends of bright and faint galaxies are likely to be related to the observed global bimodality in galaxy properties (e.g. Kauffmann et al. 2003) about a stellar characteristic stellar mass of  $\sim 3 \times 10^{10} M_\odot$ . A possible explanation could lie within the context of the hot and cold flow model of galaxy evolution (Dekel & Birnboim 2006; Kereš et al. 2005). At low masses, galaxies are able to merge and still retain their gas supply, and hence mergers would have little effect on star-formation or galaxy colours. In contrast, once galaxies merge to become more massive than a characteristic mass, shocks in the halo become stable, and preventing further cooling of gas from the halo, bringing about a transformation in the galaxy star-forming properties.

In a future article, we plan to compare our observational results with predictions from semi-analytical models of galaxy evolution applied to n-body simulations of a region containing a supercluster constrained to match the dynamical structure of the Shapley supercluster region.

## ACKNOWLEDGEMENTS

We thank the anonymous referee for helpful comments that have improved this paper. CPH, AG and NK acknowledge the financial supports provided through the European Community's Human Potential Program, under contract HPRN-CT-2002-0031 SISCO. AM is supported by the Regione Campania (L.R. 05/02) project '*Evolution of Normal and Active Galaxies*' and by the Italian Ministry of Education, University and Research (MIUR) grant COFIN2004020323: *The Evolution of Stellar Systems: a Fundamental Step Towards the Scientific Exploitation of VST*. NK is partially supported by the Italian Ministry of Education, University and Research (MIUR) grant COFIN2003020150: *Evolution of Galaxies and Cosmic Structures after the Dark Age: Observational Study*. We thank the Deep Lens Survey team and NOAO who provided the data used to derive field galaxy counts.

## REFERENCES

- Aarseth S.J., Fall S.M., 1980, ApJ, 236, 43
- Abadi M.G., Moore B., Bower R.G., 1999, MNRAS, 308, 947
- Babu G.J., Singh K., 1983, Ann. Stat., 11, 999
- Baldry I.K., Glazebrook K., Brinkmann J., Ivezić, Ž., Lupton R.H., Nichol R.C., Szalay A.S., 2004, ApJ, 600, 681
- Balogh M.L., Baldry I.K., Nichol R., Miller C., Bower R., Glazebrook K., 2004, ApJL, 615, 101
- Bardelli S., Zucca E., Zamorani G., Vettolani G., Scaramella R., 1998, MNRAS, 296, 599
- Bardelli S., Zucca E., Zamorani G., Moscardini L., Scaramella R., 2000, MNRAS, 312, 540
- Beers T.C., Flynn K., Gebhardt K., 1990, AJ, 100, 32
- Bell E.F., Wolf C., Meisenheimer K., et al. 2004, ApJ, 608, 752
- Bertin E., Arnouts S., 1996, A&AS, 331, 439
- Blanton M., Cen R., Ostriker J.P., Strauss M.A., Tegmark M., 2000, ApJ, 531, 1
- Blanton M., Hogg D.W., Bahcall N.A., et al., 2003, ApJ, 594, 186
- Blanton M., Eisenstein D., Hogg D.W., Zehavi I., 2004, ApJ in press (astro-ph/0411037)
- Blanton M., Eisenstein D., Hogg D.W., Schlegel D.J., Brinkmann J., 2005, ApJ, 629, 143
- Bruzual G., Charlot S., 2003, MNRAS, 344, 1000
- Butcher H., Oemler A., 1978, ApJ, 219, 18
- Butcher H., Oemler A., 1984, ApJ, 285, 426
- Dekel A. Birnboim Y., 2006, MNRAS, 368, 2
- Diaferio A., Kauffmann G., Balogh M.L., White S.D.M., Schade D., Ellingson E., 2001, MNRAS, 232, 999
- Dressler A., Oemler A., Butcher H., Gunn J.E., 1994, ApJ, 430, 107
- Dressler A., et al., 1997, ApJ, 490, 577
- Drinkwater M.J., Parker Q.A., Proust D., Slezak E. Quintana H., 2004, PASA, 21, 89
- Eisenstein D.J., Hogg D.W., Fukugita M., et al., 2003, ApJ, 585, 694
- Faber S.M., Willmer C.N.A., Wolf C., et al., 2005, ApJ submitted, (astro-ph/0506044)
- Finoguenov A., Henriksen M.J., Briel Y G., de Plaa J., Kaastra J.S., 2004, ApJ, 611, 811
- Fujita Y., Nagashima M., 1999, ApJ, 516, 619
- Gómez P.L., Nichol R.C., Miller C.J., et al., 2003, ApJ, 584, 210
- Ghigna S., Moore B., Governato F., Lake G., Quinn T., Stadel J., 1998, MNRAS, 300, 146
- Gray M.E., Wolf C., Meisenheimer K., Taylor A., Dye S., Borch A., Kleinheinrich M., 2004, MNRAS, 347, L73
- Haines C.P., Mercurio A., Merluzzi P., La Barbera F., Masarotti M., Busarello G., Girardi M., 2004, A&A, 425, 783
- Hogg D.W., Blanton M.R., Brinkmann J., et al., 2004, ApJL, 601, 29
- Kauffmann G., 1995, MNRAS, 274, 153
- Kauffmann G., Heckman T.M., White S.D.M., et al., 2003, MNRAS, 341, 54
- Kereš D., Katz, N., Weinberg, D.H., Davé, R. 2005, MNRAS, 363, 2
- Kodama T., Bower R.G., 2001, MNRAS, 321, 18
- Kodama T., Balogh M.L., Smail I., Bower R.G., Nakata F., 2004, MNRAS, 354, 1103
- Landolt A.U., 1992, AJ, 104, 340
- Larson R.B., Tinsley B.M., Caldwell C.N., 1980, 237, 692
- Lewis I., Balogh M., de Propris R., et al., 2002, MNRAS,

- 334, 673  
 López-Cruz O., Barkhouse, W.A., Yee H.K.C., 2004, ApJ, 614, 679  
 Mercurio A., Merluzzi P., Haines C.P., Gargiulo A., Kruzanova N., Busarello G., La Barbera F., 2006, MNRAS, 368, 109  
 Metcalfe N., Godwin J.G., Peach J.V., 1994, MNRAS, 267, 431  
 Miller N.A., 2005, AJ, 130, 2541  
 Moore B., Katz N., Lake G., Dressler A., Oemler A. Jr., 1996, Nature, 379, 613  
 Moore B., Lake G., Katz N., 1998, ApJ, 495, 139  
 Pisani A., 1993, MNRAS, 265, 706  
 Pisani A., 1996, MNRAS, 278, 697  
 Poggianti B., 1997, A&AS, 122, 399  
 Poggianti B., von der Linden, A., de Lucia, G., et al. 2006, ApJ, 642, 188  
 Quintana H., Carrasco H., Reisenegger A., 2000, AJ, 120, 511  
 Reisenegger A., Quintana H., Carrasco H., Maze, J. 2000, AJ, 120, 523  
 Roettiger K., Burns J.O., Loken C., 1996, ApJ, 473, 651  
 Shapley H., 1930, Bull. Harvard Obs., 874, 9  
 Strateva I., Ivezić Ž., Knapp G.R. et al., 2001, AJ, 122, 1861  
 Tanaka M., Goto T., Okamura S., Shimasaku K., Brinkmann J., 2004, AJ, 128, 2677  
 Thomas D., Maraston C., Bender R., Mendes de Oliveira C., 2005, ApJ, 621, 673  
 Treu T., Ellis R., Kneib J.-P., Dressler A., Smail I., Czoske O., Oemler A., Natarajan R., 2003, ApJ, 591, 53  
 Tremonti, C.A., Heckman, T.M., Kauffmann G., et al. 2004, ApJ, 613, 898  
 Vandame, 2004, PhD thesis  
 Venturi T., Bardelli S., Morganti R., Hunstead R.W., 2000, MNRAS, 314, 594  
 Wittman B.M., Tyson J.A., Dell’Antonio I.P. et al., 2002, SPIE, 4836, 73  
 Zehavi I., Zheng Z., Weinberg D.H., et al., 2005, ApJ, 630, 1